DEVELOPMENTAL BIOLOGY

Let-7 derived from endometrial extracellular vesicles is an important inducer of embryonic diapause in mice

W. M. Liu[1,2]*, R. R. Cheng[2]*, Z. R. Niu[2,3]*, A. C. Chen[2], M. Y. Ma[4], T. Li[5], P. C. Chiu[1,2], R. T. Pang[1,2], Y. L. Lee[1,2], J. P. Ou[5], Y. Q. Yao[4], W. S. B. Yeung[1,2,6†]

Copyright © 2020 The Authors, some rights reserved; exclusive licensee American Association for the Advancement of Science. No claim to original U.S. Government Works. Distributed under a Creative Commons Attribution NonCommercial License 4.0 (CC BY-NC).

Embryonic diapause is a maternally controlled phenomenon. The molecule controlling the onset of the phenomenon is unknown. We demonstrated that overexpression of microRNA let-7a or incubation with let-7g–enriched extracellular vesicles from endometrial epithelial cells prolonged the in vitro survival of mouse blastocysts, which developed into live pups after having been transferred to foster mothers. Similar to in vivo dormant blastocysts, let-7–induced dormant blastocysts exhibited low level of proliferation, apoptosis, and nutrient metabolism. Let-7 suppressed c-myc/mTORC1 and mTORC2 signaling to induce embryonic diapause. It also inhibited ODC1 expression reducing biosynthesis of polyamines, which are known to reactivate dormant embryos. Furthermore, the overexpression of let-7 blocked trophoblast differentiation and implantation potential of human embryo surrogates, and prolonged survival of human blastocysts in vitro, supporting the idea that embryonic diapause was an evolutionary conserved phenomenon. In conclusion, let-7 is the main factor inducing embryonic diapause.

INTRODUCTION

Embryonic diapause refers to a reversible arrest of the development of blastocysts. In wildlife, the phenomenon ensures that the young are born in a favorable environment. Embryonic diapause can be induced in a laboratory condition and is best studied in rodents. In mice, ovariectomy in the early morning of day 4 post-fertilization followed by progesterone administration induces embryonic diapause, during which the blastocysts become dormant and do not implant in the uterus, but can implant and develop normally when reactivated by a single dose of estradiol (*1*). A recent study showed that sheep blastocysts, which do not normally undergo embryonic diapause, could be induced to become dormant in the uterus of delayed implanting mice and could be reactivated when transferred back to the uterus of the ewe (*2*), suggesting that embryonic diapause is an evolutionary conserved phenomenon.

The onset, maintenance, and termination of embryonic diapause are under maternal control (*3*). Various factors regulate embryonic diapause. For instance, photoperiod influences embryonic diapause in minks and lactation affects that in rodents (*3*). High levels of uterine anandamide maintain embryonic diapause in mice (*4*), while the metabolite of estrogen, catechol estrogen (*5*), and polyamines (*6*) reactivates the dormant embryos in mice and mink, respectively. However, the factors that induce the onset of embryonic diapause in vivo remain unknown.

Let-7 is a family of microRNAs up-regulated in the dormant mouse blastocysts (*7*). Their expressions return to a low level after estrogen-induced reactivation (*8*). Although an overexpression of let-7a suppresses implantation (*7*), the origin and role of let-7 in the dormant blastocysts are unknown. As embryonic diapause is mainly a maternally controlled event and endometrial cells produce extracellular vesicles (EVs) containing microRNAs (*9*), we tested the hypothesis that endometrial cells produced let-7 containing EVs to induce embryonic diapause in this report. The mechanisms of the action of let-7 on embryonic diapause were investigated. In addition, we provided evidence suggesting that the actions of let-7 on embryos were conserved in humans.

RESULTS

Let-7 induces embryonic diapause

To test the hypothesis, the precursor of let-7a (pre-let-7a) or scrambled RNA (control) was electroporated into mouse blastocysts on day 4 of pregnancy. The level of mature let-7a was >40-fold higher in the pre-let-7a blastocysts than in the control blastocysts (fig. S1A). After 3 days of culture (day 7), the level of let-7a remained threefold higher in the pre-let-7a group (fig. S1A). The majority of the pre-let-7a blastocysts (95 ± 3.2%) were morphologically viable, with a large blastocoel (Fig. 1A), whereas 31 ± 2.2% of the control embryos had shrunken in size and some degenerated by that time. On day 12, over 50% of the embryos with a pre-let-7a overexpression remained morphologically viable, while all the control embryos had degenerated (Fig. 1A).

Consistent with the above observation, the percentage of apoptotic [terminal deoxynucleotidyl transferase–mediated deoxyuridine triphosphate nick end labeling–positive ($TUNEL^+$)] cells in the day 7 blastocysts ($N = 6$ embryos per group) with electroporation of pre-let-7a on day 4 (D7-let7) was significantly lower than that of the control embryos (D7-scr, $P < 0.05$; Fig. 1B). Blastocysts collected in the afternoon of day 4 of pregnancy (in vivo activated blastocysts, D4-act) had a low percentage of $TUNEL^+$ cells comparable to that of D7-let7 blastocysts (Fig. 1B).

It is well established that metabolism is suppressed in the dormant embryos (*10*). Therefore, we tested whether an overexpression of let-7a would change the energy metabolism of embryos. As expected, D7-let7 and in vivo dormant (Dor) blastocysts had low glucose

[1]Shenzhen Key Laboratory of Fertility Regulation, The University of Hong Kong-Shenzhen Hospital, Shenzhen, 1, Haiyuan 1st Road, Futian District, Shenzhen, Guangdong, P.R. China. [2]Department of Obstetrics and Gynaecology, The University of Hong Kong, Pokfulam Road, Hong Kong, P.R. China. [3]Center for Reproductive Medicine, Department of Obstetrics and Gynecology, Peking University Third Hospital, Beijing 100191, P.R. China. [4]Department of Obstetrics and Gynecology, General Hospital of Chinese People's Liberation Army, Beijing 100853, P.R. China. [5]Center for Reproductive Medicine, The Third Affiliated Hospital, Sun Yat-Sen University, No. 600 Tianhe Road, Tianhe District, Guangzhou P.R. China. [6]University of Hong Kong Shenzhen Institute of Research and Innovation, Key Laboratory Platform Building, Shenzhen Virtual University Park, No. 6, Yuexing 2nd Road, Shenzhen 518057, P.R. China.
*These authors contributed equally to this work.
†Corresponding author. Email: wsbyeung@hku.hk

Downloaded from http://advances.sciencemag.org/ on May 2, 2021

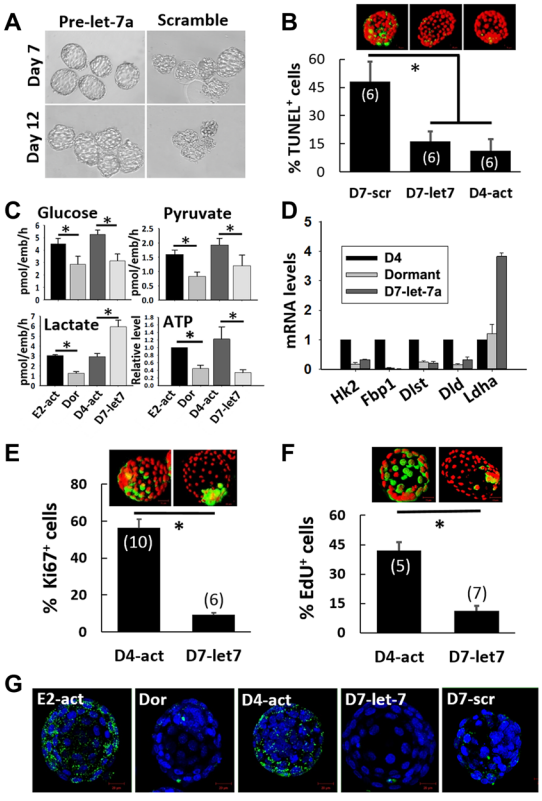

Fig. 1. Overexpression of let-7a prolongs survival of mouse blastocysts in vitro. (**A**) Overexpression of let-7a extended the survival of blastocysts in culture. Survived blastocysts were defined as those with a well-defined blastocoel. (**B**) The percentage of apoptotic cells was low in blastocysts with overexpression of let-7a on day 7 (D7-let7) and was comparable to that in day 4 activated (D4-act) blastocysts. Blastocysts electroporated with scrambled RNA (D7-scr) had significantly higher percentage of TUNEL$^+$ cells. *$P < 0.05$. (**C**) Glucose metabolism of the D7-let7 and in vivo dormant (Dor) blastocysts was low with significant reduction in glucose, pyruvate uptake, and ATP levels when compared with the D4-act blastocysts and E_2-induced reactivated blastocysts (E_2-act), respectively. D7-let7 had a high lactate production, which was low in the dormant blastocysts. *$P < 0.05$. (**D**) Expression of genes related to glucose metabolism. (**E** and **F**) The percentages of proliferating (Ki67$^+$, green) cells (E) and cells with DNA synthesis (EdU$^+$, green) (F) were lower in blastocysts of D7-let7 when compared to that in D4-act blastocysts. Numbers in parenthesis are number of embryos analyzed. *$P < 0.05$. (**G**) Dor, D7-let7, and D7-scr blastocysts did not bind significant amount of FITC-labeled EGF. The binding of EGF was high in the D4-act blastocysts and the delayed implanting mice 6 hours after E_2-act.

metabolism; their glucose, pyruvate uptakes, and adenosine triphosphate (ATP) levels were significantly lower than those of the D4-act and estrogen-induced reactivated (E_2-act) blastocysts, respectively (Fig. 1C; $N = 5$). The reduced glucose metabolism was likely a result of the inhibitory action of let-7 on its target genes related to glucose metabolism (predicted by TargetScan or RNA22), *Hk2*, *Fbp1*, *Dld*, and *Dlst* (Fig. 1D). Lactate production was unexpectedly significantly higher in the D7-let7 blastocysts than in the D4-act blastocysts (Fig. 1C), which might be due to a high level of *Ldha* (lactate dehydrogenase A) mRNA in the former (Fig. 1D).

The effects of an overexpression of let-7a on the proliferation and extent of the active DNA synthesis of blastomeres were determined by immunostaining for Ki67 and 5-ethynyl-2′-deoxyuridine (EdU) incorporation assay, respectively. The percentage of Ki67$^+$ cells in the D7-let7 blastocysts ($N = 12$) was significantly lower than that of the D4-act blastocysts ($N = 10$, $P < 0.05$; Fig. 1E). The Ki67$^+$ cells in the D7-let7 blastocysts were concentrated in the inner cell mass; this is consistent with the observation that the mouse trophectoderm cells entered dormancy earlier than the inner cell mass cells (*11*, *12*). Consistent with cell proliferation, the percentage of EdU$^+$ cells was about fourfold higher ($P < 0.05$) in the D4-act blastocysts ($N = 5$) than in the D7-let7 blastocysts ($N = 7$) (Fig. 1F). The observations were in line with the report that cell cycle arrest in the delayed implanting blastocysts occurs before the S phase (*13*).

An increase in epidermal growth factor (EGF) binding is a marker of reactivation of dormant mouse blastocysts (*5*). Dormant blastocysts did not bind a significant amount of fluorescein isothiocyanate (FITC)–labeled EGF (Dor; Fig. 1G). EGF binding was upregulated in blastocysts from delayed implanting mice at 6 hours after estradiol-induced reactivation (E_2-act). However, D7-let7 and D7-scr blastocysts exhibited a low EGF binding. The similarly low EGF binding of D7-let7 and D7-scr blastocysts could be attributed to different causes; the former reflected a diapause state, while the latter reflected a deteriorating state with many apoptotic cells (Fig. 1B).

Let-7–induced embryonic diapause is reversible

To determine whether the overexpression of let-7 in embryos had been in a reversible dormant state in vivo, a 2-fluoroestradial-17β (2-Fl-E_2)–treated mouse model was used. 2-Fl-E_2 treatment induces a receptive state of the endometrium (*5*). It also inhibits the uterine estrogen-2/4-hydroxlyase activity, thereby suppressing the synthesis of 4-hydroxy-E_2, a catechol metabolite of estradiol-17β (E_2) required for the activation of dormant mouse blastocysts (*5*). Thus, 2-Fl-E_2 injection induces uterine receptivity but fails to reactivate the dormant blastocysts in the delayed implanting mice (*5*). We transferred D7-let7 blastocysts into the 2-Fl-E_2–treated pseudo-pregnant uteri ($N = 6$ mice per group); the number of implantation sites at 28 hours after embryo transfer was significantly lower than that after the transfer of the D4-act blastocysts ($P < 0.05$; Fig. 2A).

The reversible nature of let-7–induced embryonic diapause was tested by transferring D7-let7 blastocysts into D3 pseudo-pregnant uteri. Live births were obtained from blastocysts with an overexpression of let-7a for 3 days (D7-let7) and 4 days (D8-let7; Fig. 2B). All the pups had normal birth weight (fig. S1B). No pup was born after the transfer of the D12-let7 and D7-scr blastocysts (data not shown).

In the above experiments, electroporation induced only a transient rise in the let-7a level for a few days. To determine the prolonged action of a high level of let-7 on embryo survival in vitro, we produced transgenic mice from embryonic stem cells with doxycycline (DOX)–inducible let-7g (a gift from G. Q. Daley, Harvard Stem Cell Institute, Boston, MA, USA). DOX treatment induces let-7g expression in the transgenic mice. The transgene is unique in that the loop region of the precursor let-7g (pre-let-7g) in the transgene is replaced by that of microRNA-21. Therefore, endogenous Lin28 cannot bind to pre-let-7g and block let-7g biogenesis in the transgenic mice (*14*). Let-7 family members contain a similar "seed sequence" that spans from nucleotide 2 to 8 in mice (*15*). This conserved feature suggests that the let-7 family members have similar target mRNAs and functions. Identical changes in the expression of 14 genes were observed in the blastocysts after an overexpression of let-7a and let-7g (fig. S2). The above embryo transfer experiment was repeated with the transgenic mice.

Downloaded from http://advances.sciencemag.org/ on May 2, 2021

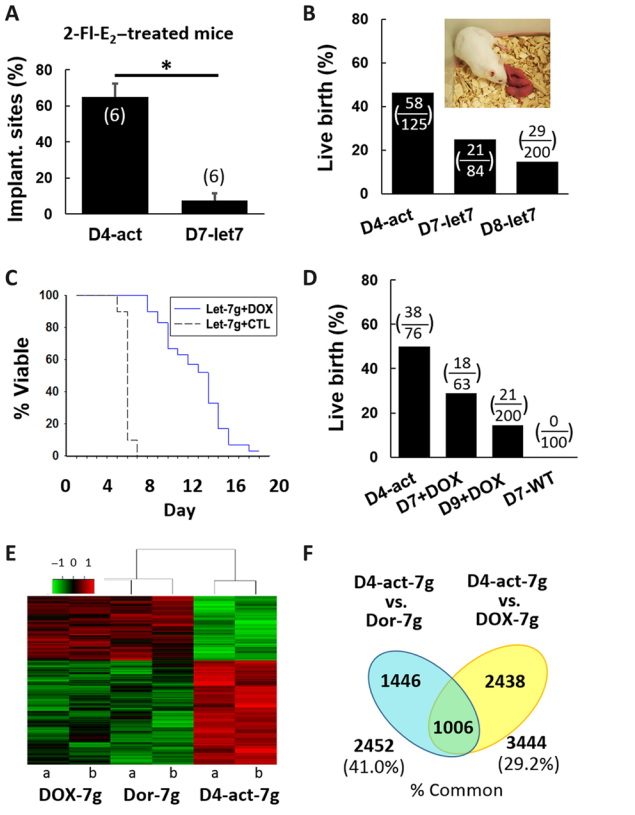

Fig. 2. Let-7–induced dormant blastocysts can be reactivated. (**A**) The implantation rate of D7-let7 after embryo transfer into 2-FI-E_2–treated mice was significantly lower than that of D4-act. 2-FI-E_2 injection induces uterine receptivity but fails to activate the dormant blastocysts in the delayed implanting mice. Numbers in parenthesis are number of animals receiving the transferred embryos. *$P < 0.05$. (**B**) Live births were obtained after transfer of blastocysts with overexpression of let-7a for 3 days (D7-let7) and 4 days (D8-let7), although the live birth rate was lower than that from D4-act blastocysts. Numbers in parenthesis are number of live birth/total number of embryos transferred. (**C**) Survival curve of blastocysts carrying an inducible let-7g transgene with and without DOX treatment cultured in KSOM + AA medium. Most of the control embryos survived until day 6, whereas 50% of the DOX-treated embryos maintained good morphology even on day 13. (**D**) Live births were obtained after transfer of let-7g blastocysts treated with DOX treatment for 3 days (D7+DOX) and 5 days (D9+DOX). No live birth was obtained from transfer of day 7 WT blastocysts. Numbers in parenthesis are number of live birth/total number of embryos transferred. (**E**) Microarray analyses of the mRNA expression of D4-act (D4-act-7g), in vitro (DOX treatment in culture, DOX-7g), and in vivo induced dormant (Dor-7g) let-7g blastocysts. Heatmap of the top 500 differentially expressed genes between the dormant and D4-act blastocysts was shown. (**F**) Venn diagram showing the number of differentially expressed genes between in vitro (DOX treatment in culture) or in vivo induced dormant blastocysts against D4-act blastocysts. Photo credit: W. M. Liu, The University of Hong Kong.

When blastocysts from the transgenic mice were treated with DOX during culture, the let-7g level in the embryos increased 32-fold, and 50% of the blastocysts survived for 14 days in vitro (Fig. 2C). Pups were obtained after the transfer of DOX-treated day 7 (D7+DOX) and day 9 (D9+DOX) blastocysts, but not day 7 wild-type (D7–WT) blastocysts, into WT day 3 pseudo-pregnant mice (Fig. 2D). Because the inducible let-7g transgenic mice better simulated the in vivo condition, their blastocysts were mainly used for subsequent experiments unless otherwise stated.

Transcriptomic analysis of let-7–induced embryos

To understand the molecular actions of let-7 on embryonic diapause, the GeneChip™ Mouse Gene 2.0 ST Array was used to determine the transcriptomes of D4-act, in vivo dormant, and let-7–induced dormant blastocysts from let-7g–transgenic mice. Unsupervised hierarchy clustering (Fig. 2E) and principal components analysis (fig. S3A) showed that the mRNA profiles (table S1) of the in vitro induced dormant blastocysts (DOX treatment in culture, DOX-7g) and the in vivo dormant blastocysts (Dor-7g) were similar but distinct from those of the D4-act let-7g blastocysts (D4-act-7g). To confirm the data obtained from the mRNA profiles, the total RNAs isolated from five pools of D4-act-7g, Dor-7g, and DOX-7g blastocysts were subjected to direct quantitative polymerase chain reaction (qPCR) analyses for the transcript levels of six genes, namely, *Ccne1*, *Btg1*, *Pkm*, *Oxct1*, *Fbp1*, and *Sap1* (fig. S3B). These genes were involved in cell cycle (*Ccne1* and *Btg1*), carbohydrate metabolism, energy pathway (*Pkm* and *Oxct1*), and chromatin remodeling (*Sap30*). The expression patterns were consistent with the results of the array. Among them, two genes (*Btg1* and *Oxct1*) were significantly higher, while the rest were significantly lower in the Dor-7g and DOX-7g blastocysts than in the D4-act-7g blastocysts ($P < 0.05$).

Compared with the D4-act-7g blastocysts, the in vitro and the in vivo induced dormant blastocysts exhibited 3444 and 2452 differentially expressed genes, respectively (Fig. 2F). Among the differentially expressed genes, 1006 of them were common in the two comparisons (Fig. 2F). Gene ontology analysis of these common genes using Database for Annotation, Visualization, and Integrated Discovery (DAVID) showed that they were related to mitotic nuclear division, cell division, G_1-S transition of mitotic cell cycle, DNA repair, DNA replication, and cell cycle (table S2).

Transfer of let-7 in uterine fluid EVs to embryos

Because embryonic diapause is a maternally regulated phenomenon, we tested the possibility of a maternal origin of let-7 in the delayed implanting blastocysts. This possibility is supported by three observations. First, transmission and scanning electron microscopy showed EV-like structures in the mouse uterine lumen (fig. S4A) and on the trophectoderm of blastocysts collected in the uterine lumen (fig. S4B), respectively. Second, immunostaining detected the presence of CD63, a marker of EVs, in the uterine epithelium of mice (fig. S4C) and on the surface of EVs from uterine luminal fluid (ULF; fig. S4D). Nanoparticle tracking analysis showed that the EVs in ULF had a mean size of 82.3 nm (fig. S4E). Western blot analysis showed that these ULF-EVs were positive for HSP70, CD63, and TSG101 and negative for calnexin and GM130. Third, mouse ULF contains let-7 carrying $CD63^+$ EVs, which can be internalized by blastocysts (*16*). To obtain further evidence, the expression patterns of let-7 in the endometrial epithelial cells, EVs from ULF (ULF-EVs), and in blastocysts from mice before embryonic diapause, during embryonic diapause, and after E_2-induced reactivation were determined. The results showed that they had similar patterns with a high let-7a expression only in the dormancy period (Fig. 3A). The pattern was markedly different from that of the stromal cells (fig. S5), supporting the idea that the endometrial epithelial cells produced EVs containing let-7a during delayed implantation.

The inducible let-7g transgenic mice carry a unique chimeric let-7g Stem/miR-21 loop sequence (S7gL21), in which the loop of pre-let-7g is replaced by that of microRNA-21. qPCR assay was developed to detect the expression of the transgene; the forward primer targeted

Downloaded from http://advances.sciencemag.org/ on May 2, 2021

on a sequence that crossed the stem and the loop of S7gL21 so that only the precursor of the transgene, but not pre-let-7g, was amplified. DOX treatment significantly induced the expression of the sequence in the liver (data not shown) and ULF-EVs (Fig. 3B, upper panel) of the transgenic mice, but not that of the ICR (Institute of Cancer Research) mice. Blastocysts from ICR mice were transferred into the pseudo-pregnant delayed implanting let-7g transgenic mice. Three days later, the expression of the S7gL21 sequence was significantly higher in the transferred embryos than in those that were not transferred (Fig. 3B, lower panel). The result confirmed that let-7 was transferred from the mother to the embryos in vivo.

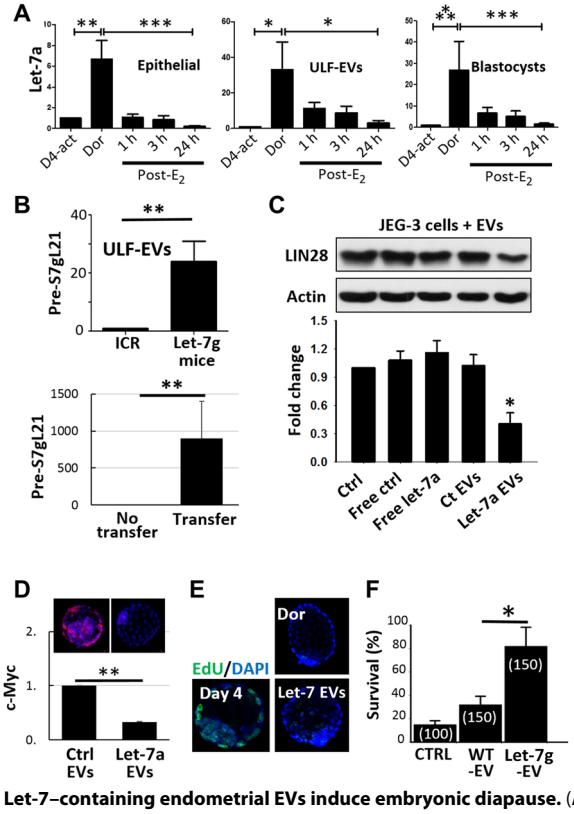

Fig. 3. Let-7–containing endometrial EVs induce embryonic diapause. (**A**) The expression patterns of let-7a in endometrium epithelial cells, EVs of ULF-EVs, and blastocysts in the mouse delayed implantation model before and during diapause and 1, 3, and 24 hours after estradiol-induced reactivation were similar. *$P < 0.05$; **$P < 0.01$; ***$P < 0.001$. (**B**) The expression of pre-S7gL21 was significantly higher in ULF-EVs from DOX-treated transgenic mice carrying an inducible let-7g transgene relative to that of ICR mice (upper panel) and in ICR blastocysts after transfer into the DOX-treated let-7g transgenic mice when compared to ICR blastocysts without transfer (lower panel). **$P < 0.01$. (**C**) Let-7 in EVs suppressed the level of LIN28 in human trophoblast JEG-3 cells. Let-7a–containing EVs generated by transfection of endometrial cells with pre-let-7a, but not EV-free let-7a, suppressed expression of LIN28. *$P < 0.05$. (**D** and **E**) Let-7a–enriched EVs suppressed expression of c-myc protein (D) and DNA synthesis (E) in day 4 mouse blastocysts. Day 4 embryos were cocultured with let-7a–enriched EVs or control EVs. Expression of c-myc protein (green) was observed by confocal microscopy after immunohistochemical staining and analyzed with the ImageJ software ($n = 15$ embryos for each group). DNA synthesis was determined by EdU incorporation assay. Green, newly synthesized DNA; blue, DAPI. $n = 20$ embryos for each group. **$P < 0.01$. (**F**) Let-7g–enriched EVs from DOX-treated endometrial epithelial cells of let-7g transgenic mice (Let-7g-EV) prolonged the survival of WT day 4 blastocysts in KSOM + AA medium. The survival rate on day 7 of untreated blastocysts and those treated with EVs from WT mice was low. Numbers in parenthesis are number of embryos analyzed. *$P < 0.05$.

To study the biological effect of let-7a and let-7g in EVs, we produced let-7–enriched EVs by two methods. First, let-7a–enriched EVs were isolated from the spent culture medium of human endometrial Ishikawa cells transfected with pre-let-7a. Transfection with scrambled RNA was used as control. The collected EVs at physiological concentration were then used to treat day 4 blastocysts or human trophoblast JEG-3 cells. Endometrial EVs containing let-7a, but not EV-free let-7a, were biologically active in suppressing the expression of let-7 targets, LIN28A [lin-28 homolog A (*Caenorhabditis elegans*); Fig. 3C], C-MYC (MYC proto-oncogene), and RICTOR (RPTOR independent companion of MTOR, complex 2; fig. S5B) in the JEG-3 cells. Incubation of the let-7a–enriched EVs for 24 hours significantly decreased the protein expression of c-myc in the treated blastocysts relative to the control embryos (Fig. 3D) and reduced their DNA synthesis (let-7 EVs; Fig. 3E) to a level comparable to that in the in vivo dormant blastocysts (Dor; Fig. 3E).

To better simulate the in vivo situation, let-7g–enriched EVs were obtained from endometrial epithelial cells of let-7g transgenic mice treated with DOX for 4 days in a medium supplemented with 10% EV-free fetal bovine serum (FBS) and were used at physiological concentration to treat WT day 4 blastocysts in KSOM + amino acid (AA) medium. After 3 days of culture, 82 ± 16.2% ($N = 150$) of the let-7g-EV–treated blastocysts still had the blastocoel, and 12 ± 5.4% of them developed to term after an embryo transfer. In contrast, 85 ± 10.1% ($N = 100$) of the blastocysts degraded in the absence of EVs (Fig. 3F), and the survived ones produced no pups after transfer.

Let-7 is upstream of mTOR and c-myc signaling in delayed implanting blastocysts

Inhibition of mTOR (mammalian target of rapamycin) (*17*) or MYC (*18*) induces a diapause-like state in mouse embryos. We consistently observed significant decreases in the transcript expression of c-myc and *Akt1* (mTOR activator) and increases in that of *Tsc1* and *Tsc2* (mTOR inhibitors) in the let-7g–induced dormant blastocysts when compared with the untreated blastocysts (Fig. 4A). On the other hand, *Pten* of PIK3 (phosphatidylinositol-3-kinase) signaling, an upstream pathway of mTOR, was unaffected by the DOX treatment.

Next, we determined whether *c-myc* mediated the action of let-7g on the induction of embryonic diapause. In vitro transcription was used to generate *c-myc* mRNA. The mRNA was biologically active, and the level of C-MYC protein in the JEG-3 cells increased fourfold at 24 hours after transfection of the mRNA (Fig. 4B). Electroporation of the *c-myc* mRNA enhanced C-MYC expression (fig. S6A) and EdU incorporation (Fig. 4C) in D4 blastocysts. Overexpression of *c-myc* also nullified the effects of let-7g overexpression on the prolongation of the embryo survival in vitro; in the presence of DOX, the let-7g transgenic blastocysts transfected with *c-myc* mRNA could only survive until day 6; the vast majority died the next day, whereas 50% of the DOX-treated transgenic blastocysts without the transfection survived up to day 15 (fig. S6B).

C-MYC is upstream of mTORC1 in rat fibroblasts (*19*). The incubation of JEG-3 cells with an inhibitor of mTORC1/mTORC2 pathways, INK-128, for 24 hours reduced phosphorylation of mTORC1 target and RpS6 phosphorylated at $Ser^{235/236}$ (pRpS6) and had no effect on the expression of C-MYC (Fig. 4D). On the other hand, treatment with the C-MYC inhibitor 10058-F4 [MYC inhibitor (MI)] (*20*) significantly decreased the phosphorylation of mTORC1 targets, pRpS6, and p4EBP1 (4EBP1 phosphorylated at $Thr^{37/46}$) in

Downloaded from http://advances.sciencemag.org/ on May 2, 2021

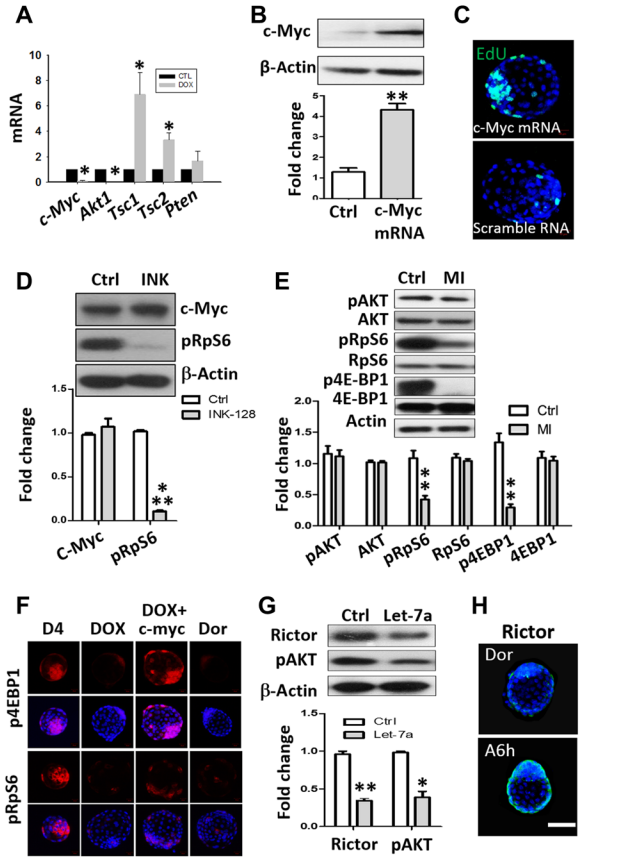

Fig. 4. Molecular mechanism of let-7–induced diapause. (**A**) RT-PCR analysis showing the expression of c-myc and mTOR signaling components after let-7g overexpression. D4 blastocysts from let-7g transgenic mice were cultured in the presence or absence of DOX for 48 hours before determination of gene expression. *$P < 0.05$. (**B**) Expression of c-myc in JEG-3 trophoblast cells at 24 hours after transfection of c-myc mRNA. **$P < 0.01$. (**C**) Representative confocal images of EdU incorporation (green) in blastocysts at 24 hours after electroporation of c-myc mRNAs or scrambled RNA. Blue, nuclei. Scale bar, 50 μm. (**D**) Expression of c-Myc and pRpS6 in JEG-3 cells treated with mTOR inhibitor, INK-128, for 24 hours. ***$P < 0.001$. (**E**) Western blot analysis of the effect of c-myc inhibitor 10058-F4 (MI) on mTORC1 targets (pRpS6 and p4EBP1) and mTORC2 target (pAKT) in JEG-3 cells. All quantification measurements are normalized to β-actin. **$P < 0.01$. (**F**) Representative confocal images of blastocysts immunostained for p4EBP1 and pRpS6. D4 blastocysts from let-7g transgenic mice were electroporated with or without c-myc mRNA before culture in the presence or absence of DOX. ICR D4 blastocysts (D4) and dormant embryos (Dor) served as positive and negative controls, respectively. (**G**) Expression of Rictor and phosphorylated AKT protein in JEG-3 cells transfected with either let-7a mimics or scramble for 24 hours. Data are presented as means ± SE. *$P < 0.05$; **$P < 0.01$. (**H**) Representative confocal microscope images showing Rictor in embryos during diapause and at 6-hour post–estrogen-induced reactivation (A6h). Scale bar, 50 μm.

the JEG-3 cells (Fig. 4E) and D4 blastocysts (fig. S6C). The phosphorylation level of mTORC2 target, AKT at Ser^{473} (pAKT), was unexpectedly not affected (Fig. 4E and fig. S6C), suggesting that mTORC1, but not mTORC2, signaling was downstream of C-MYC in blastocysts and trophoblast cells. Overexpression of *c-myc* mRNA in day 4 let-7g blastocysts for 48 hours reduced the inhibitory effects of DOX-induced let-7g on mTORC1 targets (Fig. 4F).

Inhibition of mTORC1 alone was insufficient to induce embryonic diapause (*17*). Therefore, bioinformatics analysis was conducted to find whether let-7 also targeted the mTORC2 pathway. TargetScan identified that a component of mTORC2, *Rictor*, was a potential target of let-7. The prediction was supported by the down-regulation of RICTOR expression in the JEG-3 cells at 48 hours after transfection of the cells with pre-let-7a (Fig. 4G). Dual luciferase assay confirmed that *Rictor* was a direct target of let-7a. At 24 hours after transfection, let-7a mimics reduced the luciferase activity of *Rictor* 3′ untranslated region (3′UTR) reporter by about fivefold when compared to the scramble control (fig. S7). Mutation of the let-7a binding sites on the reporter construct abolished the reduction in luciferase activity (fig. S7). As expected, the expression of RICTOR was lower in the dormant embryos (Dor) than in those at 6-hour post–E_2-induced reactivation (A6h; Fig. 4H). The action of let-7 on mTORC2 signaling was further confirmed by a significant decrease in pAKT expression in the JEG-3 cells at 48 hours after transfection of pre-let-7a when compared with the scramble control (Fig. 4G).

Let-7 inhibits production of polyamines

The inhibition of polyamine biosynthesis delays the reactivation of dormant embryos in vitro (*21*). We consistently found an increased expression of polyamine biosynthesis enzymes, ornithine decarboxylase (ODC1) and spermine synthesis enzyme (SMS) in the reactivated embryos (A24h), relative to the dormant embryos (Dor; Fig. 5A).

Odc1 encodes a rate-limiting enzyme in polyamine biosynthesis. An analysis of a genome-wide embryonic C-MYC chromatin immunoprecipitation (ChIP) sequencing dataset (*22*) revealed recruitment of C-MYC at the promoter of *Odc1* and identified five putative c-myc response elements on the promoter (Fig. 5B). Luciferase reporter assays showed that response elements 3, 4, and 5 were the major sites that conferred C-MYC responsiveness (Fig. 5B). Site-specific ChIP assays using the DNA from mouse primary uterine epithelial cells isolated from delayed implanting (Dor-ME) and day 4 activated mouse uteri (D4-act) confirmed the recruitment of C-MYC to these response elements (Fig. 5C). There were reductions in the recruitment of C-MYC to these elements of *Odc1* promoter in the uterine epithelial cells during embryonic diapause (Dor-ME) when compared to those from D4-act mice (Fig. 5C).

Our data further showed that the inhibition of C-MYC by MI for 24 hours significantly decreased the protein level of ODC1 in the JEG-3 cells (Fig. 5D) and D4 blastocysts (Fig. 5E). Treatment with DOX reduced the protein expression of ODC1 in the let-7g blastocysts relative to the D4 blastocysts (Fig. 5F). The action was mediated by C-MYC as the transfection of *c-myc* mRNA abolished the let-7–induced down-regulation of ODC1 in the embryos (Fig. 5F). Together, endometrial epithelial cell–derived let-7 suppressed c-myc/mTORC1, mTORC2 signaling, and polyamine biosynthesis to induce embryonic diapause (Fig. 5G).

Let-7–enriched EVs modulate human blastocyst development and implantation

Non-diapause sheep blastocysts become dormant in the uteri of delayed implanting mice and can be reactivated after a transfer to the uterus of ewe (*2*). We tested whether let-7–enriched EVs would affect the differentiation of a human embryo surrogate model termed BAP-EB (*23*). BAP-EB was derived by BAP (BMP4, A83-01, and PD173074)–induced differentiation of embryoid bodies of human embryonic stem cells (hESCs) into trophoblast spheroids. BAP-EB spheroids resemble human blastocysts in size and morphology. They express markers of trophectoderm and trophoblast and do not express those of other germ layers. BAP-EB selectively attached onto

Downloaded from http://advances.sciencemag.org/ on May 2, 2021

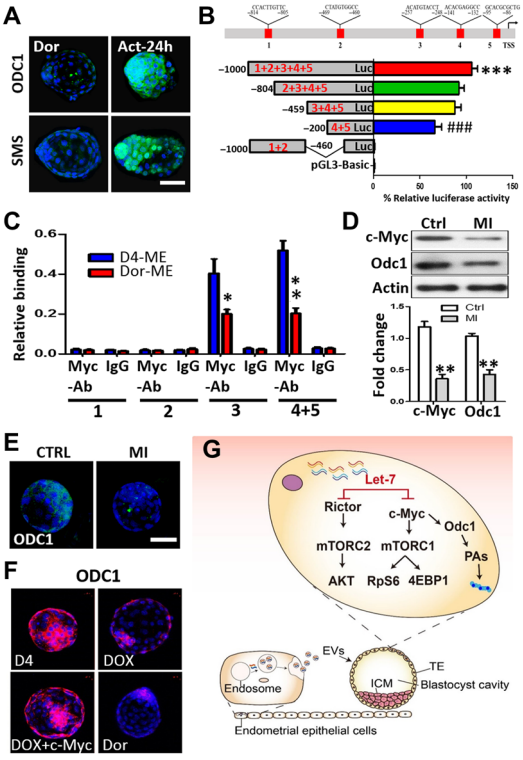

Fig. 5. Let-7 inhibits polyamine synthesis. (**A**) Representative confocal microscope images of Dor and Act-24h embryos immunostained for ODC1 and SMS. Scale bar, 50 μm. (**B**) Schematic representation of the five putative myc response elements in the proximal *Odc1* promoter (upper). Luciferase activities in 293T cells after cotransfection of a *c-myc* expression vector with empty luciferase reporter (pGL3) and long or short *Odc1* promoter constructs (lower). Data represent means ± SE. ***$P < 0.001$ versus empty reporter (pGL3); ###$P < 0.001$ versus long *Odc1* promoter construct. (**C**) ChIP-qPCR assay to evaluate the relative myc binding to the *Odc1* promoter isolated from uterine epithelial cells on day 4 of pregnancy (D4-ME) and during diapause (Dor-ME). Amplified putative myc response elements (1, 2, 3, and 4-5) are depicted in the upper panel of (B). Data represent means ± SE. *$P < 0.05$ and **$P < 0.01$. (**D** and **E**) The expression of ODC1 was detected at 24 hours after incubation with or without the c-myc inhibitor 10058-F4 (MI) in JEG-3 trophoblast cells (D) and in blastocysts (E). All quantification measurements in Western blot were normalized to β-actin. Scale bar, 50 μm. (**F**) D4 blastocysts from let-7g transgenic mice were electroporated with or without c-myc mRNA before culture in the presence of DOX. D4 and Dor blastocysts served as positive and negative controls, respectively. (**G**) Schematic diagram summarizing the molecular actions of endometrium-derived let-7 in inducing embryonic diapause. Blastocysts take up endometrial EVs enriched with let-7. Let-7 inhibits c-myc, leading to reduction of mTORC1 activity and reduction in ODC1 biosynthesis. Polyamines are required for reactivation of diapausing embryo. Let-7 also suppresses mTORC2 directly by its action on mTORC2 component *Rictor*.

primary receptive endometrial epithelial cells and receptive endometrial epithelial cell lines, but not other nonendometrial cell lines, nonreceptive endometrial cell line, and primary prereceptive endometrial epithelial cells (*23*).

The time when BAP was added to induce trophoblast differentiation was considered as time zero of post-induction of differentiation (pid). During differentiation, the expression of the marker of inner cell mass (*OCT4*) in the BAP-EB spheroids decreased rapidly at 48-hour pid and was undetectable by 96-hour pid. The expression pattern was different from that of the trophectoderm and trophoblast markers. The trophectoderm marker (*CDX2*) showed a transient increase at 48-hour pid, while those of trophoblast (*CK7*, *CDH1*, and *GATA2*), syncytiotrophoblast (*ERVW-1* and *CGB*), and extravillous trophoblast (*MMP2* and *HLA-G*) increased progressively with differentiation. Treatment with let-7g-EVs at 48-hour pid significantly affected the mRNA expression of these trophoblast markers at 96-hour pid relative to the control-EV–treated spheroids (Fig. 6A); let-7–treated BAP-EB at 96-hour pid exhibited significantly higher levels of trophectoderm marker (*CDX2*) and lower levels of trophoblastic markers (*GATA2*, *CK7*, *CDH1*, *ERVW-1*, *CGB*, *MMP2*, and *HLA-G*). The comparable expression levels of these markers in the let-7g-EV–treated spheroids at 96-hour pid with that of the spheroids at 48-hour pid were consistent with a high level of let-7–induced dormancy and cessation of differentiation.

BAP-EB spheroids attach specifically onto receptive endometrial cells resembling the early implantation event (*23*). Treatment with let-7g-EVs reduced the protein expression of c-myc (fig. S8) in the BAP-EB and significantly decreased their attachment onto the receptive endometrial epithelial Ishikawa cells ($P < 0.05$; Fig. 6B).

Good quality human blastocysts can be obtained in 65% of the cultured blastocysts on day 5 and 30% on day 6, but only 5% on day 7 (*24*). In this study, day 5 human blastocysts ($N = 21$) were treated with let-7g–enriched EVs and their viability in terms of the presence of a blastocoel, morphology of the trophectoderm cells, and the inner cell mass cells were examined. The blastocoel and good morphology were maintained in 52% of let-7g-EV–treated blastocysts on day 7, whereas only 30% did so in the untreated group ($N = 10$). One of the EV-treated blastocysts remained viable until day 8 (Fig. 6C). The observations were consistent with a beneficial effect of let-7 on embryo survival in vitro.

DISCUSSION

There have long been efforts searching for the natural initiator of embryonic diapause but without much success. Our data show that let-7 of endometrial epithelial origin is a key inducer of embryonic diapause in vivo. Specifically, when the mice undergo diapause, the endometrium generates let-7–enriched EVs, which are taken up by blastocysts. Two observations support the role of let-7 in the induction of embryonic diapause. First, the overexpression of let-7a and incubation with let-7–enriched EVs prolonged blastocyst survival in vitro. Second, the treated embryos developed to term after an embryo transfer. The study further demonstrates a conserved action of let-7 on the induction of diapause-like phenotype in a human embryo surrogate and the prolongation of survival of human embryos in vitro.

Let-7 is a key inducer of embryonic diapause because it can simultaneously regulate the two known pathways leading to embryonic diapause. Two recent studies showed that simultaneous inhibition of C-MYC and N-MYC (*18*) or inhibition of mTORC1 and mTORC2 (*17*) signaling is required for the induction of embryonic diapause. The present data showed that let-7 induced embryonic diapause via the inhibition of both the C-MYC/mTORC1 and mTORC2 signaling pathways. Although the action of let-7 on *n*-myc has not been studied, it is known that there are two let-7 binding sites in the 3′UTR of *Mycn* (*25*). Therefore, it is likely that let-7 also suppresses the expression of *n-myc*.

Let-7 inhibits *Odc1* expression via the suppression of *c-myc*. This can be a mechanism reducing the potential of diapausing

Downloaded from http://advances.sciencemag.org/ on May 2, 2021

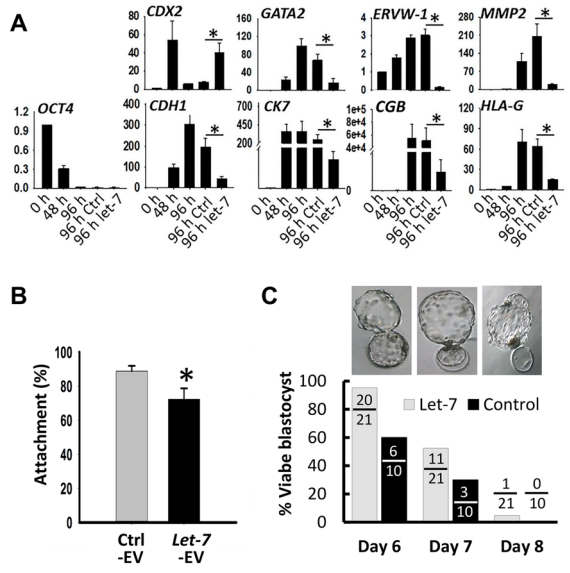

Fig. 6. Effects of let-7–enriched EVs on human embryos and their surrogates. (**A**) Treatment of hESC-derived trophoblast spheroids (BAP-EB, human embryo surrogates) with Let-7g–enriched EVs at 48-hour pid significantly reduced the mRNA expression of trophoblast [*CK7* (keratin 7), *CDH1* (cadherin 1), and *GATA2* (GATA-binding protein 2)], syncytiotrophoblast [*ERVW-1* (endogenous retrovirus group W member 1, envelope) and *CGB* (chorionic gonadotropin subunit beta 3)], and extravillous trophoblast [*MMP2* (matrix metallopeptidase 2) and *HLA-G* (major histocompatibility complex, class I, G)] markers at 96-hour pid relative to the control EV–treated BAP-EB. The expression of pluripotent genes [*OCT4* (POU class 5 homeobox 1) and *CDX2* (caudal type homeobox 2)] decreased within this period. $^*P < 0.05$. (**B**) Treatment with let-7g–enriched EVs significantly reduced the attachment of BAP-EB onto receptive endometrial epithelial cells, Ishikawa. At 48-hour pid of BAP-EB, control EVs or Let-7g–enriched EVs were incubated with BAP-EB until 72-hour pid; the spheroids were evenly transferred onto a confluent monolayer of Ishikawa cells and further cocultured for 3 hours. Nonadherent spheroids were removed, and the percentage of attached BAP-EB was calculated. $^*P < 0.05$. (**C**) Viability of day 5 human blastocysts after treatment with let-7–enriched EVs or control EVs for 3 days. Blastocysts with a blastocoel were considered viable.

blastocysts to be reactivated, as polyamine biosynthesis is required for reactivation, and inhibition of their biosynthesis in embryos delays reactivation in vitro (*21*). Our site-specific ChIP assay demonstrated a reduced recruitment of C-MYC to the *Odc1* promoter during diapause. Whether the reduction is due to the suppression of C-MYC expression resulting from a high expression of let-7 in the cells during diapause remains to be determined.

We localized the C-MYC protein mainly to the cytoplasm of embryos. This differs from the expected nuclear localization of C-MYC in many cell types. The antibody used in this report localized the expression of C-MYC to the nuclei of embryonic stem cells (fig. S6D). Three other anti–C-MYC antibodies were tested and showed similar cytoplasmic C-MYC expression in embryos (data not shown). The expression of cytoplasmic MYC has been reported. MYC-nick is a cytoplasmic cleavage product of the full-length C-MYC, widely expressed in a large number of cell lines (*26*). It is expressed in differentiating cells and tissues and plays a significant role in the differentiation of myofibroblasts and the transdifferentiation of fibroblasts into muscle cells (*26*). Thus, a let-7–induced decrease of cytoplasmic C-MYC may lead to a decrease in the differentiation potential of the diapausing blastocysts.

Let-7 overexpression induced dormancy via the suppression of apoptosis, cell proliferation, DNA synthesis, and energy metabolism. The majority of these phenotypes can be explained by the actions of let-7 on its targets, for instance, a high level of let-7 targets on *c-myc* to inhibit proliferation (*27*), caspase-3 to suppress apoptosis (*28*), and HK2 to reduce glucose utilization (*29*). A high let-7 expression is also associated with the quiescence of fibroblasts (*30*). Our results on *Hk2* and *Fbp1* mRNA expression are in contrast with those of a previous proteomic study (*31*). The discrepancies could possibly be due to different comparisons made in the two studies: dormant versus reactivated blastocysts at 12 to 14 hours after E_2 injection in the previous studies but dormant versus D4 activated blastocysts in the present study.

Contrary to the low lactate production of dormant embryos in vivo, an overexpression of let-7 up-regulated lactate production. *Dld* and *Dlst* are *let-7* targets. They are subunits of the 2-oxo-glutarate complex and the α-ketoglutarate dehydrogenase complex of carbohydrate metabolism. Inhibition of DLD (Dihydrolipoamide dehydrogenase) activity in spermatozoa causes lactate accumulation (*32*), and infantile lactic acidosis is associated with severe deficiencies of the α-ketoglutarate dehydrogenase complex (*33*). These conditions may have been recapitulated in the present model by the suppressive action of *let-7* on *Dld* and *Dlst*. Alternatively, the observation could be due to an indirect action of let-7 on *Ldha* via its well-known target *Lin28a*. Overexpression of *Lin28a* decreases the expression of *Ldha* in the human embryonic kidney cells (*34*). The molecular mechanism of *Lin28a* on the observation remains to be determined.

Transcriptomic analyses showed that the mRNA profile of let-7g–induced embryonic diapause is about 30 to 40% similar to that of in vivo dormant embryos. These common genes represent the let-7–affected genes contributing to in vivo–induced embryonic diapause. Consistently, gene ontology analysis of the common genes showed that they were related to pathways expected to be involved in embryonic diapause. The present study demonstrates that ULF-EVs are important in the induction of embryonic diapause. EVs contain many other components. The lack of some of these components could explain the differential expression of genes between the let-7g–induced and in vivo dormant embryos. The differentially expressed genes may be responsible for the phenotypes that are different between the let-7–induced and the in vivo embryonic diapause, such as high lactate production after let-7–induced embryonic diapause. Their absence may also explain the inability of an overexpression of let-7 alone in maintaining the survival of embryos for a very long term.

The endometrium produces ULF-EVs containing proteins, mRNAs, and microRNAs that are believed to be important means of communication between the blastocysts and the endometrium (*9*). Let-7 containing EVs inhibited the differentiation of human embryo surrogates and reduced their attachment onto receptive endometrial epithelial cells. Dysregulation of endometrial microRNAs occurs in subfertile women (*35*). It is possible that an abnormal expression of embryonic diapause-related microRNAs in the endometrial-derived EVs would retard the differentiation of the implanting embryos, leading to asynchronous development between the embryos and the endometrium. Desynchronization in the development between the blastocyst and the endometrium is a cause of implantation failure (*36*). However, further studies are required to explore this possibility.

Downloaded from http://advances.sciencemag.org/ on May 2, 2021

In conclusion, the study showed an important role of endometrial EVs in embryo dormancy, demonstrating that let-7 in EVs is a major player in the induction of embryonic diapause.

MATERIALS AND METHODS

A summary of the techniques and procedures for addressing the questions raised in the report can be found in the Supplementary Materials.

Use of animals

The study protocol was approved by the Committee on the Use of Live Animals in Teaching and Research, The University of Hong Kong (CULATR number: 3560-15). Females of the ICR mice were mainly used. Transgenic mice carrying a DOX-inducible let-7g gene (Slet-7gLmiR-21) were generated by the injection of embryonic stem cells carrying the let-7gStem/21loop sequence (a gift from G. Daley, Harvard Stem Cell Institute, Boston, MA, USA) into ICR blastocysts. The chimeric mice generated were then bred with CD-1 females to generate germline-transmitted pups. To match the genetic background of the embryonic stem cells carrying the transgene (V6.5 mESC), the mouse line was maintained on a C57/B6 background by backcrossing more than five times.

Collection of mouse embryos

ICR female mice aged 6 to 8 weeks were superovulated by successive intraperitoneal injections of 5 IU of pregnant mare serum gonadotropin (Sigma-Aldrich, St. Louis, USA) and 5 IU of human chorionic gonadotropin (hCG; Sigma-Aldrich) 47 to 48 hours apart and were mated with male mice. The vaginal plug was checked the day following mating. The day when a vaginal plug was seen was considered as day 1 of pregnancy. Blastocysts were collected from the uteri at 96 hours after hCG injection and cultured in M16 medium (Sigma-Aldrich) or KSOM + AA medium (Millipore, MA, USA). In normal pregnancy, blastocysts are activated by an estradiol surge in the afternoon of day 4 of pregnancy.

Delayed implanting mice were generated as reported (*7*). Briefly, pregnant mice were ovariectomized in the morning (8:00 a.m. to 9:00 a.m.) of day 4 followed by daily subcutaneous injection of progesterone (P_4; 2 mg per mouse; Sigma-Aldrich) from days 5 to 7 (*5*) to maintain the delayed implantation status. Dormant blastocysts were activated by a single subcutaneous injection of E_2 (25 ng per mouse; Sigma-Aldrich) into the delayed implanting mice on day 7 of pregnancy.

Embryo transfer

Female mice were mated with vasectomized males to generate pseudopregnant mice. Embryos were flushed out on day 4 of pregnancy and cultured as described above. Before embryo transfer, the mice were anesthetized with pentobarbital (40 mg/kg, intraperitoneally). Twenty embryos were transferred to each mouse. The implantation sites on day 5 of pregnancy were identified by intravenous injection of 0.1 ml of 1% Chicago blue dye (Sigma-Aldrich) in saline, or the numbers of live birth were recorded.

Collection and isolation of endometrial cells

Endometrial epithelial and stromal cells were isolated after the collection of ULF. Briefly, the uteri were opened longitudinally, and the tissues were digested in trypsin (Difco, BD Biosciences, MD, USA) for 1.5 hours at 4°C and then for 30 min at 37°C. Dulbecco's modified Eagle's medium (DMEM)/F12 medium (Sigma-Aldrich) supplemented with 10% FBS (Thermo Fisher Scientific, CA, USA) was used to stop the digestion. The epithelial cells were collected after a gentle shaking to separate the cells from the uterine tissues and were washed with phosphate-buffered saline (PBS) thrice at 300*g* for 10 min. The cells were then cultured briefly for 30 min to remove the contaminated stromal cells before reseeding to another culture well for experimentation. The remaining tissues were further digested by collagenase I (10 mg/ml; Invitrogen, Carlsbad, USA) and deoxyribonuclease (DNase; 5 mg/ml; Invitrogen) for 30 min with shaking at 37°C. After stopping the digestion as described above, the stromal cells were shaken from the tissues. The cell pellets collected were washed by PBS thrice and filtered through a nylon mesh with pore size of 40 μm (BD Falcon Co., NJ, USA) before RNA isolation. The purity of the epithelial cells and stromal cells was over 90% as determined by immunostaining, using antibodies against mouse cytokeratin (Dako, Glostrup, Denmark) and mouse CD90 (BD Biosciences, MA, USA), respectively.

Manipulation of let-7 levels in embryos

Electroporation

Pre-let-7a or scrambled miRNA control (Thermo Fisher Scientific) was electroporated into day 4 blastocysts from ICR mice as described (*7*). Briefly, the uteri of day 4 pregnant mice were flushed with Hank's solution to obtain blastocysts, which were then transferred to prewarmed droplets of M16 medium. Pre-let-7a or scramble control was electroporated into the embryos in a flat electrode chamber (1-mm gap between electrodes; BTX Inc., San Diego, USA) in 20 μl of Hepes-buffered saline (150 mM NaCl, 20 mM Hepes, Sigma-Aldrich), by two sets of three electric pulses of 1 ms at 30 V with 1-min interval between sets, and inverting polarity using the 830 Electro Square Porator (BTX Inc., San Diego, USA). Following electroporation, the embryos were cultured in KSOM + AA or M16 for experimentation. About 95% of the electroporated embryos survived the process; they showed no sign of cell lysis at 2 hours after electroporation.

Treatment with let-7–enriched EV

Ishikawa cells were transfected with pre-let-7a or pre-miR scramble using Lipofectamine 2000 (Thermo Fisher Scientific). After transfection, the transfection medium was replaced by fresh MEM medium supplemented with 1% penicillin/streptomycin, 1% L-glutamine, and 10% EV-depleted FBS (Thermo Fisher Scientific, CA, USA). The spent medium after 48 hours of culture was collected for EV isolation. EVs were isolated from the spent medium with the Total Exosome Isolation Kit (Thermo Fisher Scientific) according to the manufacturer's instruction. The let-7a levels in the EVs were detected by reverse transcription qPCR (RT- qPCR) (let-7a primer, Thermo Fisher Scientific). Alternatively, let-7g–enriched EVs were isolated from the spent medium after culture of DOX-treated endometrial epithelial cells from the let-7g transgenic mice in medium supplemented with 10% EV-depleted FBS for 48 hours. The epithelial cells with a purity of more than 90% were isolated as above. The protein concentration of the EV preparation was determined with the BCA Protein Assay Kit (Thermo Fisher Scientific) with a working concentration range of 5 to 2000 μg/ml. The let-7–enriched EVs at a final concentration of 100 μg/ml were used for coincubation with embryos.

Downloaded from http://advances.sciencemag.org/ on May 2, 2021

Isolation of EVs from ULF

Pregnant mice or delayed implanting mice at 3, 6, and 24 hours after E_2 reactivation were sacrificed by an overdose of pentobarbital (150 to 200 mg/kg, intraperitoneally). Their uteri were isolated, and ULF was collected by flushing the uterine lumen with 500 μl of PBS. The embryos in the flushing were removed under a dissection microscopy. EVs in the ULF were isolated with the Total Exosome Isolation Kit. Briefly, the ULF was centrifuged successively at 300*g* for 10 min to remove cells, at 2000*g* for 10 min to remove dead cells, and at 20,000*g* for 60 min to remove cell debris and large vesicles. The pellets that formed in each centrifugation were discarded. After the last centrifugation, the total exosome isolation reagent (250-μl volumes) was mixed with the supernatant overnight at 4°C on a roller mixer, before the samples were centrifuged at 10,000*g* for 60 min at 4°C. The supernatant was discarded, and the ULF-EV pellet was gently washed once with 200 μl of PBS to remove residual extract buffer and resuspended in 20 μl of PBS and stored at −80°C. The size and purity of the isolated ULF-EVs were determined using a nanoparticle tracking analyzer (ZetaView PMX 120, Particle Metrix, Germany), electron microscopy (FEI Tecnai G2 20 Scanning TEM, FEI Co., USA), and Western blot analysis of EV-specific markers HSP70 (Abcam, Cambridge, UK), CD63 (Abcam), and TSG101 (Abcam) and negative control markers GM130 (Abcam) and calnexin (Abcam), as described (*16*). The average protein content of pooled ULF-EV preparations was 1.2 ± 0.2 μg per mice as determined with the BCA Protein Assay Kit (Thermo Fisher Scientific). The volume of mouse ULF on days 2 to 5 of pseudo-pregnancy is 2 to 5 μl per mice (*37*). Therefore, the protein concentration of EV in ULF was estimated to be 240 to 600 μg/ml in vivo. In this study, embryos were treated with EVs at a physiological dose of 100 μg/ml.

TUNEL assay

Cell apoptosis was examined with the In Situ Cell Death Detection Kit (Roche Diagnostics GmbH, Mannheim, Germany) according to the manufacturer's instruction. Briefly, embryos were fixed in 4% paraformaldehyde for 15 min at room temperature, permeabilized with 0.1% Triton X-100 in Dulbecco's PBS (DPBS) for 30 min, and then incubated with TUNEL reaction mixture containing 5 μl of enzyme solution and 45 μl of label solution at 37°C for 60 min. The embryos were washed three times with PBS. Their nuclei were stained with propidium iodide (Sigma-Aldrich) for 5 min before the embryos were mounted on microscope slides for examination under a fluorescence-inverted microscope (TE300; Nikon, Japan).

Metabolite analysis

The method used was a miniaturized version of conventional enzymatic methods, which rely on the detection of ultraviolet (UV)–excited NADH (reduced form of nicotinamide adenine dinucleotide) and NADPH (reduced form of nicotinamide adenine dinucleotide phosphate) in enzyme coupled reactions (*38*). Instead of having the enzymatic reactions conducted in cuvettes, they were done in 20-μl droplets on a petri dish. The specific enzyme cocktails for the metabolite studied were as follows: glucose cocktail: 42 mM EPP S (4-(2-Hydroxyethyl)-1-piperazinepropanesulfonic acid) buffer (pH 8.0), 42 μM dithiothreitol, 3 mM $MgSO_4{\cdot}7H_2O$, 0.42 mM ATP, 1.2 mM NADP, and hexokinase (14 U/ml)/glucose-6-phosphate dehydrogenase (7 U/ml; Roche Applied Science); pyruvate cocktail: 63 mM EPP buffer (pH 8.0), 0.1 mM NADH, and L-lactate dehydrogenase (75 U/ml; Roche Applied Science); lactate cocktail: 0.45 M glycine/0.73 M hydrazine buffer, 4.5 mM NAD, and L-lactate dehydrogenase (69 U/ml; Roche Applied Science).

The cocktail droplet (2 μl) was mixed with 18 μl of spent culture media. Following a 3-min incubation at room temperature, 5 μl of the medium was transferred to a homemade chamber with a chamber depth of 1 mm, and its fluorescence intensity was determined under a fluorescence microscope. The fluorescence signal relative to the background was determined by the pixel intensities using the Image-Pro Plus 6.0 software (Media Cybernetics Inc., Silver Spring, MD, USA). The background signal was estimated using a method described previously (*39*). The changes in fluorescence were converted to changes in the concentration based on standard curves performed on the same day with known concentrations of the appropriate substrates.

EdU incorporation assay

DNA synthesis was determined by the EdU incorporation assay (Thermo Fisher Scientific) according to the manufacturer's instruction. Briefly, embryos were cultured in KSOM medium containing 10 μM EdU for 30 min before washing with PBS. After the removal of the zona pellucida, the embryos were fixed in methanol at −20°C for 20 min and permeated in PBS containing 1% bovine serum albumin (BSA) and 0.5% Triton X-100. The incorporated EdU was detected by incubation with 1 mM $CuSO_4$ and 100 μM fluorescent azide for 30 min. The staining mixture was prepared fresh each time. The embryos were washed three times with PBS containing 0.05% Tween 20 before the fluorescence signal was visualized under a confocal microscope (Carl Zeiss LSM 700, Zeiss, Germany).

Immunofluorescence staining of embryos

The embryos were washed with M2 medium (Sigma-Aldrich) and fixed in 4% paraformaldehyde for 15 min at room temperature. They were permeabilized with 0.1% Triton X-100 in DPBS for 30 min and incubated for 1 hour in DPBS containing 1% BSA at room temperature before incubation with antibodies against C-MYC, pAKT, pRpS6, p4EBP1 (Abcam, UK), or Ki67 (Santa Cruz Biotechnology Inc., Santa Cruz, CA) at 4°C overnight followed by incubation with secondary antibody [FITC-labeled anti-goat immunoglobulin G (IgG)] for 1 hour at 37°C. Nuclei were stained with 4′,6-diamidino-2-phenylindole (DAPI) (5 μg/ml; Sigma-Aldrich) or propidium iodide (1 μg/ml) for 5 min. Last, the embryos were rinsed in DPBS to remove excess reagents and examined under a confocal microscope.

Western blot analysis

Proteins were extracted from the JEG-3 cells and the uterine epithelial cells with radioimmunoprecipitation assay (RIPA) lysis buffer supplemented with protein inhibitor and phosphatase inhibitors (Sigma-Aldrich). The concentration of proteins in the extract was measured using the BCA Kit (Thermo Fisher Scientific). The protein extracts were separated on 10% SDS–polyacrylamide gel electrophoresis, transferred onto polyvinylidene difluoride membranes (Merck Millipore, Germany), and probed with antibodies against c-myc (Cell Signaling Technology, MA, USA), ODC1, SMS, pAKT, p4EBP1, pRpS6, and the total protein of AKT, 4EBP1, and RpS6 (Cell Signaling Technology). β-Actin (Sigma-Aldrich) was used as the internal control. The membranes were incubated with the WesternBright ECL Kit (Advansta, CA, USA) and exposed to x-ray films.

Downloaded from http://advances.sciencemag.org/ on May 2, 2021

Extraction of total RNA from embryos

Embryos at the same developmental stage were randomly pooled into three groups with five embryos per group. Total RNA was extracted from each group in 0.5 μl of 2 M guanidine isothiocyanate (Sigma-Aldrich) buffer at room temperature for 5 min. Complete lysis of the embryos in the buffer was confirmed under a microscope. The samples were diluted to 5 μl with double-distilled water and were used directly for the multiplex microRNA assays.

Precursor-microRNA primer design for Slet-7gLmiR-21

To amplify the precursor-microRNA, the forward and reverse primers were designed to anneal to the stem portion of the hairpin. The forward primer was designed for a sequence that crossed the stem and the loop of the precursor of Slet-7gLmiR-21 so that only its stem, but not that of the pre-let-7g, was amplified. The sequences of the primers used for pre-S7gL21 were as follows: forward: 5′-GTAGTAGTTTGTACAGTTCTGT-3′; reverse: 5′-TAAATCCTGGCAAGGC-3′; probe: 5′-CTGTACAGTCCATGAGATT-3′; Rt reverse: 5′-TAAATCCTGGCAAGGCA-3′.

Structure of Slet-7gLmiR-21 in the transgenic mouse

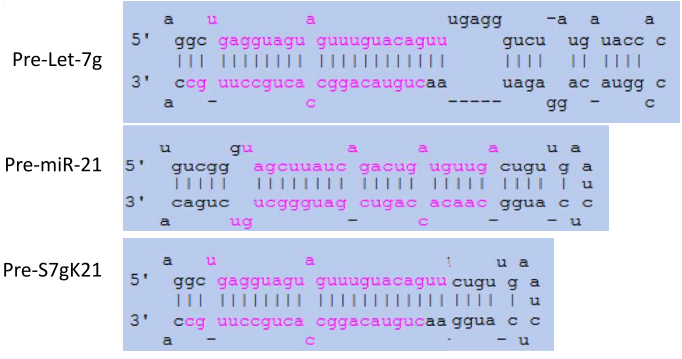

Precursor-microRNA detection in mouse embryos

Embryos were lysed in 5% NP-40 to release the total RNA. RT primer annealing was performed at 85°C for 5 min by adding 1 pmol of RT reverse primer to 1 μg of the above RNA. Then, the samples were placed immediately in ice to avoid the formation of stem-and-loop structure. RT was performed at 45°C for 60 min and at 85°C for 5 min and then kept at 4°C in a thermal cycler (T100 Thermal Cycler, Bio-Rad, CA, USA). RT-qPCR was performed with the 7500 Real-Time PCR System (Thermo Fisher Scientific). The program was a 10-min cycle at 95°C, followed by 45 cycles of 15 s at 95°C and 60 s at 60°C.

Microarray

Microarray (GeneChip™ Mouse Gene 2.0 ST) was used to study the effect of let-7 overexpression on the transcriptome of the treated blastocysts. For each sample, RNA was collected from 10 blastocysts. RNA extraction, amplification, and purification were performed according to Kurimoto *et al.* (*40*). The complementary DNAs (cDNAs) from day 7 dormant blastocysts, D4-act, and DOX-induced blastocysts were hybridized to the GeneChip™ Mouse Gene 2.0 ST array in duplicates (Affymetrix, CA, USA). All cDNA hybridizations were performed by the Centre for Genomic Sciences, The University of Hong Kong. The microarray data have been deposited to the Gene Expression Omnibus (GSE141900). The data were analyzed using Partek Genomics Suite 6.6 (St. Louis, MO, USA). The expression matrix was further subjected to the R package linear models for microarray data (*41*) for identifying the differentially expressed genes. Principal components were computed and plotted with the R packages FactoMineR and factoextra. Heatmaps were plotted with the R package gplots using *z* scores calculated for each gene across different samples. Biological process analysis was performed by DAVID (v6.8) (*42*).

Preparation of c-myc mRNA

To obtain the DNA template for in vitro transcription, the pcDNA 3.1_cMyc plasmid containing the coding DNA sequence was PCR-amplified using the following primers: 5′-TAATACGACTCACTATAGATGCCCCTCAACGTGAAC-3′ (with T7 polymerase promoter) and 5′-TTATGCACCAGAGTTTCGAAGC-3′. The product was purified using the GeneJET PCR Purification Kit (Thermo Fisher Scientific). The MEGAscript T7 ULTRA Transcription Kit (Thermo Fisher Scientific) was used for in vitro transcription from DNA to mRNA according to the manufacturer's instructions. Briefly, DNA template was recovered at a final concentration of 1 μg/μl. Transcription reaction was performed by incubation at 37°C for 4 hours. TURBO DNase (1 μl) was added into the reaction and incubated for 15 min at 37°C before the addition of the tailing reagents for poly(A) tailing. Last, RNA was recovered using phenol:chloroform extraction and isopropanol precipitation. The recovered RNA was then quantified and stored at −80°C and was ready for transfection.

Dual luciferase assay

The mouse genomic DNA was extracted from the ICR mouse liver using a DNA extraction kit (Thermo Fisher Scientific) according to the manufacturer's protocol. The 3′UTR of *Rictor* was amplified with the Not I and Xho I digestion sites by the Phusion High Fidelity DNA Polymerase (New England Biolabs, Beverly, MA, USA). The PCR products were first purified with the GeneJET PCR Purification Kit (Thermo Fisher Scientific), digested with the Not I and Xho I enzymes (New England Biolabs), and purified with the GeneJET PCR Purification Kit again. The purified PCR products were ligated with the Not I– and Xho I–digested psiCHECK-2 vector (Promega, WI, USA). Lipofectamine 2000 transfection reagent (Thermo Fisher Scientific) was used to cotransfect 1 μg of the WT and mutant (Mut) reporter constructs with 5 nM let-7a mimic (Thermo Fisher Scientific) into a monolayer of JEG-3 cells at 70% confluence in Opti-MEM (Thermo Fisher Scientific). At 24 hours after transfection, the cells were lysed in 100 μl of 1× passive lysis buffer (Promega). The luciferase assays were performed using a luciferase assay kit (Promega) according to the manufacturer's protocol and were measured using a luminometer (GloMax 96 Microplate Luminometer, Promega). Renilla luciferase was used for normalization.

ChIP assay

ChIP analysis was performed using the Pierce Chromatin Prep Module (Thermo Fisher Scientific, 26158) according to the manufacturer's instruction. Uterine epithelium cells from delayed implanting and activated mice were isolated as described above. Formaldehyde was used to cross-link DNA and its interacting proteins in the cells. The cells were then lysed in the Lysis Buffer on ice for 10 min and centrifuged. The supernatant was discarded, while the nuclei were

Downloaded from http://advances.sciencemag.org/ on May 2, 2021

Table 1. The primer sequences used for ChIP. The data obtained were normalized to the input [fold differences = $2^{-(Ct\ sample - Ct\ input)}$].

Promoter	Forward primers	Reverse primers
Odc1-1	CCAATACTGAATATGTAAGTC	TGCGAACAGAGTCTGGGCAG
Odc1-2	GGGCTTGTCTCTCAGCAAGCTT	GATGGGCCGTGAGCTGTGCGC
Odc1-3	GTTCAGCCGTTAGGACCTGGAG	TCACCAGTCCTGGCTGCCAGCAT
Odc1-4 and Odc1-5	GTGTCCTAGGCGGAGAGGTAG	ACCACATCACCAGTCCTGGCTGC

resuspended in the MNase Digestion Buffer. Micrococcal nuclease was added to digest the chromatin. Immunoprecipitation was performed with the ChIP-grade c-Myc antibody (Cell Signaling Technology) at a dilution of 1:100. Proteinase K was used to disrupt the cross-links between the DNA and proteins. The DNA was then purified using the PCR Cleanup Extraction Kit (Thermo Fisher Scientific), after which quantitative RT-PCR was performed with the SYBR Green Master Mix (Thermo Fisher Scientific) using the following ChIP primer sequences (Table 1).

EGF binding assay

Blastocysts were incubated for 10 min at 37°C in an atmosphere of 5% CO_2 in 40-μl microdrops of M16 containing Alexa Fluor 488–labeled EGF (2 μg/ml; Thermo Fisher Scientific). Unlabeled EGF peptide at a concentration of 20 μg/ml was used as control for nonspecific binding of the labeled peptide. After termination of the incubation, blastocysts were washed in medium and fixed in 4% paraformaldehyde in PBS for 15 min at 4°C. *Z*-stack images of fixed embryos were captured with a confocal fluorescence microscope (Carl Zeiss LSM700, Germany). For quantification of the EGF binding, the images of the embryos were analyzed with the ImageJ software (1.52p, USA). The average fluorescence intensity was calculated. The data presented were the averages of the fluorescence intensity from at least three embryos.

Human trophoblastic spheroid (BAP-EB) formation and attachment assay

BAP-EB spheroids were generated from hESCs as described (*23*). Briefly, hESCs (VAL3, Spanish Stem Cell Bank, Spain) were digested to single cells with accutase (Thermo Fisher Scientific, Waltham, USA) and aggregated in AggreWellTM400 (STEMCELL Technologies Inc., Canada) in mTeSRTM1 medium (STEMCELL Technologies Inc., Canada) for 24 hours before the induction of trophoblast differentiation in BAP medium (mouse embryonic fibroblast–conditioned medium supplemented with BMP4 (10 ng/ml; R&D Systems, Minneapolis, USA), 1 μM A83-01 (Stemgent, San Diego, USA), and 0.1 μM PD173074 (Stemgent). The medium was changed daily during a 96-hour differentiation.

Control EVs or let7-enriched EVs were added to the BAP-EB culture at 48-hour pid. For the attachment assay, BAP-EB at 72-hour pid was transferred onto a confluent monolayer of Ishikawa cells and cocultured for 3 hours. Nonadherent spheroids were removed, and the percentage of attached BAP-EB was determined. For the gene expression analyses, BAP-EB at 0 and 48 hours before EV treatments and BAP-EB at 96 hours after EV treatments were collected and subjected to total RNA extraction and real-time quantification of marker expressions, as described (*23*).

Human embryos

Human embryos were obtained from infertile couples attending the assisted reproduction clinics at the Department of Obstetrics and Gynecology, General Hospital of Chinese People's Liberation Army and the Center for Reproductive Medicine, The Third Affiliated Hospital, Sun Yat-Sen University. The Institutional Review Board of the Hospital approved the project (S2017-095-01), and written consent was obtained from each donor. The embryos were donated because the donor couples had completed their family ($N = 17$), or the embryos were chromosomal abnormal as determined by preimplantation genetic testing for aneuploidy ($N = 4$). The donated embryos were cryopreserved on day 5 before experimentation.

EVs were obtained from endometrial cells of let-7g transgenic mice after treatment with DOX in DMEM/F12 medium supplemented with EV-free FBS for 4 days. Control EVs were obtained from cells without DOX treatment. On the day of experimentation, the donated blastocysts were thawed and cultured in G2 medium (Vitrolife, Sweden) supplemented with let-7g–enrched EVs or control EVs until they were morphologically not viable.

Data analysis

All the results are shown as means ± SEM. All the data were analyzed using one-way analysis of variance (ANOVA). A *P* value of less than 0.05 was considered statistically significant.

SUPPLEMENTARY MATERIALS

Supplementary material for this article is available at http://advances.sciencemag.org/cgi/content/full/6/37/eaaz7070/DC1

View/request a protocol for this paper from *Bio-protocol*.

REFERENCES AND NOTES

1. S. K. Dey, H. Lim, S. K. Das, J. Reese, B. C. Paria, T. Daikoku, H. Wang, Molecular cues to implantation. *Endocr. Rev.* **25**, 341–373 (2004).
2. G. E. Ptak, E. Tacconi, M. Czernik, P. Toschi, J. A. Modlinski, P. Loi, Embryonic diapause is conserved across mammals. *PLOS ONE* **7**, e33027 (2012).
3. J. C. Fenelon, A. Banerjee, B. D. Murphy, Embryonic diapause: Development on hold. *Int. J. Dev. Biol.* **58**, 163–174 (2014).
4. H. Wang, H. Matsumoto, Y. Guo, B. C. Paria, R. L. Roberts, S. K. Dey, Differential G protein-coupled cannabinoid receptor signaling by anandamide directs blastocyst activation for implantation. *Proc. Natl. Acad. Sci. U.S.A.* **100**, 14914–14919 (2003).
5. B. C. Paria, H. Lim, X.-N. Wang, J. Liehr, S. K. Das, S. K. Dey, Coordination of differential effects of primary estrogen and catecholestrogen on two distinct targets mediates embryo implantation in the mouse. *Endocrinology* **139**, 5235–5246 (1998).
6. P. L. Lefèvre, M.-F. Palin, G. Chen, G. Turecki, B. D. Murphy, Polyamines are implicated in the emergence of the embryo from obligate diapause. *Endocrinology* **152**, 1627–1639 (2011).
7. W.-M. Liu, R. T. K. Pang, A. W. Y. Cheong, E. H. Y. Ng, K. Lao, K.-F. Lee, W. S. B. Yeung, Involvement of microRNA lethal-7a in the regulation of embryo implantation in mice. *PLOS ONE* **7**, e37039 (2012).

Downloaded from http://advances.sciencemag.org/ on May 2, 2021

8. A. W. Cheong, R. T. K. Pang, W.-M. Liu, K. S. A. Kottawatta, K.-F. Lee, W. S. B. Yeung, MicroRNA Let-7a and dicer are important in the activation and implantation of delayed implanting mouse embryos. *Hum. Reprod.* **29**, 750–762 (2014).
9. Y. H. Ng, S. Rome, A. Jalabert, A. Forterre, H. Singh, C. L. Hincks, L. A. Salamonsen, Endometrial exosomes/microvesicles in the uterine microenvironment: A new paradigm for embryo-endometrial cross talk at implantation. *PLOS ONE* **8**, e58502 (2013).
10. H. M. Weitlauf, Metabolic changes in the blastocysts of mice and rats during delayed implantation. *J. Reprod. Fertil.* **39**, 213–224 (1974).
11. C. Kamemizu, T. Fujimori, Distinct dormancy progression depending on embryonic regions during mouse embryonic diapause. *Biol. Reprod.* **100**, 1204–1214 (2019).
12. R. L. Given, DNA synthesis in the mouse blastocyst during the beginning of delayed implantation. *J. Exp. Zool.* **248**, 365–370 (1988).
13. M. I. Sherman, P. W. Barlow, Deoxyribonucleic acid content in delayed mouse blastocysts. *J. Reprod. Fertil.* **29**, 123–126 (1972).
14. H. Zhu, N. Shyh-Chang, A. V. Segrè, G. Shinoda, S. P. Shah, W. S. Einhorn, A. Takeuchi, J. M. Engreitz, J. P. Hagan, M. G. Kharas, A. Urbach, J. E. Thornton, R. Triboulet, R. I. Gregory; DIAGRAM Consortium; MAGIC Investigators, D. Altshuler, G. Q. Daley, The *Lin28/let-7* axis regulates glucose metabolism. *Cell* **147**, 81–94 (2011).
15. H. Lee, S. Han, C. S. Kwon, D. Lee, Biogenesis and regulation of the *let-7* miRNAs and their functional implications. *Protein Cell* **7**, 100–113 (2016).
16. Z. Niu, R. T. K. Pang, W. Liu, Q. Li, R. Cheng, W. S. B. Yeung, Polymer-based precipitation preserves biological activities of extracellular vesicles from an endometrial cell line. *PLOS ONE* **12**, e0186534 (2017).
17. A. Bulut-Karslioglu, S. Biechele, H. Jin, T. A. Macrae, M. Hejna, M. Gertsenstein, J. S. Song, M. Ramalho-Santos, Inhibition of mTOR induces a paused pluripotent state. *Nature* **540**, 119–123 (2016).
18. R. Scognamiglio, N. Cabezas-Wallscheid, M. C. Thier, S. Altamura, A. Reyes, Á. M. Prendergast, D. Baumgärtner, L. S. Carnevalli, A. Atzberger, S. Haas, L. von Paleske, T. Boroviak, P. Wörsdörfer, M. A. G. Essers, U. Kloz, R. N. Eisenman, F. Edenhofer, P. Bertone, W. Huber, F. van der Hoeven, A. Smith, A. Trumpp, Myc depletion induces a pluripotent dormant state mimicking diapause. *Cell* **164**, 668–680 (2016).
19. E. V. Schmidt, M. J. Ravitz, L. Chen, M. Lynch, Growth controls connect: Interactions between c-myc and the tuberous sclerosis complex-mTOR pathway. *Cell Cycle* **8**, 1344–1351 (2009).
20. M.-J. Huang, Y.-c. Cheng, C.-R. Liu, S. Lin, H. E. Liu, A small-molecule c-Myc inhibitor, 10058-F4, induces cell-cycle arrest, apoptosis, and myeloid differentiation of human acute myeloid leukemia. *Exp. Hematol.* **34**, 1480–1489 (2006).
21. L. J. Van Winkle, A. L. Campione, Effect of inhibitors of polyamine synthesis on activation of diapausing mouse blastocysts in vitro. *J. Reprod. Fertil.* **68**, 437–444 (1983).
22. L. Fagnocchi, A. Cherubini, H. Hatsuda, A. Fasciani, S. Mazzoleni, V. Poli, V. Berno, R. L. Rossi, R. Reinbold, M. Endele, T. Schroeder, M. Rocchigiani, Ż. Szkarłat, S. Oliviero, S. Dalton, A. Zippo, A Myc-driven self-reinforcing regulatory network maintains mouse embryonic stem cell identity. *Nat. Commun.* **7**, 11903 (2016).
23. Y.-L. Lee, S.-W. Fong, A. C. H. Chen, T. Li, C. Yue, C.-L. Lee, E. H. Y. Ng, W. S. B. Yeung, K.-F. Lee, Establishment of a novel human embryonic stem cell-derived trophoblastic spheroid implantation model. *Hum. Reprod.* **30**, 2614–2626 (2015).
24. E. R. Hammond, L. M. Cree, D. E. Morbeck, Should extended blastocyst culture include day 7? *Hum. Reprod.* **33**, 991–997 (2018).
25. J. T. Powers, K. M. Tsanov, D. S. Pearson, F. Roels, C. S. Spina, R. Ebright, M. Seligson, Y. de Soysa, P. Cahan, J. Theißen, H.-C. Tu, A. Han, K. C. Kurek, G. S. LaPier, J. K. Osborne, S. J. Ross, M. Cesana, J. J. Collins, F. Berthold, G. Q. Daley, Multiple mechanisms disrupt the *let-7* microRNA family in neuroblastoma. *Nature* **535**, 246–251 (2016).
26. M. Conacci-Sorrell, C. Ngouenet, R. N. Eisenman, Myc-nick: A cytoplasmic cleavage product of Myc that promotes α-tubulin acetylation and cell differentiation. *Cell* **142**, 480–493 (2010).
27. T.-C. Chang, L. R. Zeitels, H.-W. Hwang, R. R. Chivukula, E. A. Wentzel, M. Dews, J. Jung, P. Gao, C. V. Dang, M. A. Beer, A. Thomas-Tikhonenko, J. T. Mendell, Lin-28B transactivation is necessary for Myc-mediated let-7 repression and proliferation. *Proc. Natl. Acad. Sci. U.S.A.* **106**, 3384–3389 (2009).
28. W. P. Tsang, T. T. Kwok, Let-7a microRNA suppresses therapeutics-induced cancer cell death by targeting caspase-3. *Apoptosis* **13**, 1215–1222 (2008).
29. S. Jiang, W. Yan, S. E. Wang, D. Baltimore, Let-7 suppresses B cell activation through restricting the availability of necessary nutrients. *Cell Metab.* **27**, 393–403.e4 (2018).
30. E. J. Suh, M. Y. Remillard, A. Legesse-Miller, E. L. Johnson, J. M. S. Lemons, T. R. Chapman, J. J. Forman, M. Kojima, E. S. Silberman, H. A. Coller, A microRNA network regulates proliferative timing and extracellular matrix synthesis during cellular quiescence in fibroblasts. *Genome Biol.* **13**, R121 (2012).
31. Z. Fu, B. Wang, S. Wang, W. Wu, Q. Wang, Y. Chen, S. Kong, J. Lu, Z. Tang, H. Ran, Z. Tu, B. He, S. Zhang, Q. Chen, W. Jin, E. Duan, H. Wang, Y.-L. Wang, L. Li, F. Wang, S. Gao, H. Wang, Integral proteomic analysis of blastocysts reveals key molecular machinery governing embryonic diapause and reactivation for implantation in mice. *Biol. Reprod.* **90**, 52 (2014).
32. S. Panneerdoss, A. B. Siva, D. B. Kameshwari, N. Rangaraj, S. Shivaji, Association of lactate, intracellular pH, and intracellular calcium during capacitation and acrosome reaction: Contribution of hamster sperm dihydrolipoamide dehydrogenase, the E3 subunit of pyruvate dehydrogenase complex. *J. Androl.* **33**, 699–710 (2012).
33. K.-F. Sheu, J. P. Blass, The α-ketoglutarate dehydrogenase complex. *Ann. N. Y. Acad. Sci.* **893**, 61–78 (1999).
34. C. K. Docherty, I. P. Salt, J. R. Mercer, Lin28A induces energetic switching to glycolytic metabolism in human embryonic kidney cells. *Stem Cell Res. Ther.* **7**, 78 (2016).
35. Y. Choi, H.-R. Kim, E. J. Lim, M. Park, J. A. Yoon, Y. S. Kim, E.-K. Kim, J. E. Shin, J. H. Kim, H. Kwon, H. Song, D.-H. Choi, Integrative analyses of uterine transcriptome and MicroRNAome reveal compromised LIF-STAT3 signaling and progesterone response in the endometrium of patients with recurrent/repeated implantation failure (RIF). *PLOS ONE* **11**, e0157696 (2016).
36. J. Bellver, C. Simón, Implantation failure of endometrial origin: What is new? *Curr. Opin. Obstet. Gynecol.* **30**, 229–236 (2018).
37. R. G. Wales, W. R. Edirisinghe, Volume of fluid and concentration of cations and energy substrates in the uteri of mice during early pseudopregnancy. *Reprod. Fertil. Dev.* **1**, 171–178 (1989).
38. J. P. Urbanski, M. T. Johnson, D. D. Craig, D. L. Potter, D. K. Gardner, T. Thorsen, Noninvasive metabolic profiling using microfluidics for analysis of single preimplantation embryos. *Anal. Chem.* **80**, 6500–6507 (2008).
39. T. Bernas, D. Barnes, E. K. Asem, J. P. Robinson, B. Rajwa, Precision of light intensity measurement in biological optical microscopy. *J. Microsc.* **226**, 163–174 (2007).
40. K. Kurimoto, Y. Yabuta, Y. Ohinata, M. Saitou, Global single-cell cDNA amplification to provide a template for representative high-density oligonucleotide microarray analysis. *Nat. Protoc.* **2**, 739–752 (2007).
41. M. E. Ritchie, B. Phipson, D. Wu, Y. Hu, C. W. Law, W. Shi, G. K. Smyth, *limma* powers differential expression analyses for RNA-sequencing and microarray studies. *Nucleic Acids Res.* **43**, e47 (2015).
42. D. W. Huang, B. T. Sherman, R. A. Lempicki, Bioinformatics enrichment tools: Paths toward the comprehensive functional analysis of large gene lists. *Nucleic Acids Res.* **37**, 1–13 (2009).

Acknowledgments

Funding: The project is supported by a grant from the National Natural Science Foundation of China (NSFC 31471398); a grant from the Research Grant Council (GRF 17107915), Hong Kong; and a National Key Basic Research Development Program (973 Program) from the Ministry of Science and Technology of the People's Republic of China (MOST 2018YFC1004402) to W.S.B.Y. **Author contributions:** Conceptualization: W.S.B.Y., W.M.L., and R.R.C.; conduct of the experiments: W.M.L., R.R.C., Z.R.N., M.Y.M., T.L., P.C.C., and R.T.P.; data analysis: W.S.B.Y., Y.L.L., W.M.L., and A.C.C.; writing (original draft): W.S.B.Y. and W.M.L.; writing (review and editing): all authors. **Competing interests:** The authors declare that they have no competing interests. **Data and materials availability:** All data needed to evaluate the conclusions in the paper are present in the paper and/or the Supplementary Materials. The microarray data have been deposited to the Gene Expression Omnibus. Additional data available from W.S.B.Y. upon request.

Submitted 3 October 2019
Accepted 27 July 2020
Published 9 September 2020
10.1126/sciadv.aaz7070

Citation: W. M. Liu, R. R. Cheng, Z. R. Niu, A. C. Chen, M. Y. Ma, T. Li, P. C. Chiu, R. T. Pang, Y. L. Lee, J. P. Ou, Y. Q. Yao, W. S. B. Yeung, Let-7 derived from endometrial extracellular vesicles is an important inducer of embryonic diapause in mice. *Sci. Adv.* **6**, eaaz7070 (2020).

Downloaded from http://advances.sciencemag.org/ on May 2, 2021

Science Advances

Let-7 derived from endometrial extracellular vesicles is an important inducer of embryonic diapause in mice

W. M. Liu, R. R. Cheng, Z. R. Niu, A. C. Chen, M. Y. Ma, T. Li, P. C. Chiu, R. T. Pang, Y. L. Lee, J. P. Ou, Y. Q. Yao and W. S. B. Yeung

Sci Adv **6** (37), eaaz7070.
DOI: 10.1126/sciadv.aaz7070

ARTICLE TOOLS http://advances.sciencemag.org/content/6/37/eaaz7070

SUPPLEMENTARY MATERIALS http://advances.sciencemag.org/content/suppl/2020/09/04/6.37.eaaz7070.DC1

REFERENCES This article cites 42 articles, 5 of which you can access for free
http://advances.sciencemag.org/content/6/37/eaaz7070#BIBL

PERMISSIONS http://www.sciencemag.org/help/reprints-and-permissions

Use of this article is subject to the Terms of Service

Science Advances (ISSN 2375-2548) is published by the American Association for the Advancement of Science, 1200 New York Avenue NW, Washington, DC 20005. The title *Science Advances* is a registered trademark of AAAS.

Copyright © 2020 The Authors, some rights reserved; exclusive licensee American Association for the Advancement of Science. No claim to original U.S. Government Works. Distributed under a Creative Commons Attribution NonCommercial License 4.0 (CC BY-NC).

Downloaded from http://advances.sciencemag.org/ on May 2, 2021